

## $O(\alpha_s^2)$ mass contributions to the $H$ dibaryon in a truncated bag model

Eugene Golowich and Thomas Sotirelis

*Department of Physics and Astronomy, University of Massachusetts, Amherst, Massachusetts 01003*

(Received 4 November 1991)

The  $H$  dibaryon is a color-singlet flavor-singlet spinless six-quark configuration. We discuss aspects of its Fock-space wave vector in the quark model and discuss construction of diquark state vectors as well. We then address the general issue of computing higher-order contributions to mass. A formalism is developed, and calculations are carried out in a truncated bag model. Mass contributions to both diquark systems and the  $H$  dibaryon are computed to  $O(\alpha_s^2)$ .

PACS number(s): 14.20.Pt, 12.40.Aa

### I. INTRODUCTION

The QCD Lagrangian gives little hint as to the physical spectrum of the real world. The zero-coupling limit of free quarks and gluons bears no resemblance to the observed collection of hadrons. Despite many years of effort, direct attempts to unravel the mystery of QCD dynamics have met with limited success.

As a consequence, one often seeks alternative means to better understand the inner workings of QCD. A potentially fruitful approach is to combine theoretical analysis with input from experiment. Such is the case regarding theoretical and experimental searches for states lying beyond the well-studied  $Q\bar{Q}$  and  $Q^3$  configurations of the quark model. In this paper we shall consider two such configurations: the six-quark composites called "dibaryons" and the two-quark composites called "diquarks." We shall discuss each of these objects in some detail presently. It suffices here to note that theoretical insights regarding these structures have, for the most part, been obtained as a result of calculations which are of *first* order in the strong fine-structure constant  $\alpha_s$ . On this basis it is believed that the lightest dibaryon is the so-called  $H$  (see below) and that the most tightly bound diquark configuration is the spin-zero color and flavor antitriplet.

It is our primary aim in this paper to report on an investigation of  $O(\alpha_s^2)$  mass contributions to  $Q^6$  and  $Q^2$  configurations. For definiteness, throughout, we employ spatial wave functions of the bag model and work in the "truncation" approximation, which considers only the lowest-energy quark and gluon modes. We begin in Sec. II by considering aspects of six-quark state vectors and then, in Sec. III, review the construction of diquark states. A formalism for computing higher-order energy contributions is discussed in Sec. IV A, specifics of the truncation approximation to the bag model are addressed in Sec. IV B, and the calculations themselves are described in Sec. IV C. Finally, we summarize the significance of our findings in Sec. V.

### II. $H$ DIBARYON

#### A. Six-quark representation

The only six-quark configuration known unambiguously to exist in nature is the deuteron. In this case color correlations between the constituent quarks produce a loosely bound moleculelike bound state of two distinct baryons. It is an open question whether there can also exist objects in which six quarks have highly similar spatial wave functions. We follow convention in referring to such hypothetical configurations as "dibaryons." Quark-model formulations of the problem have yielded conflicting results, both positive [1] and negative [2]. Additional dynamical contributions such as the effect of instanton-induced effects [3] have also been studied. Although there are reports consistent with detection of a dibaryon [4], the present situation is quite confused.

Table I lists the spectroscopy of all possible color-singlet six-quark configuration of ground-state (i.e.,  $S$ -wave) quarks [1]. Observe that the list of allowed states is a remarkably restrictive one in that the spin-zero states can occur only in the SU(3)-flavor representation 1, 27, and 28. The 28 is of little phenomenological interest because it does not occur in the Clebsch-Gordan series of two SU(3) octets, and so none of its states occur as resonances or bound states in baryon-baryon channels. At the other extreme the SU(3) singlet state, commonly referred to as the  $H$  dibaryon, has been the subject of the

TABLE I. Spectroscopy of six-quark configurations.

SU(6) of color spin	SU(3) of flavor	Spin
490	1	0
896	8	1,2
280	10	1
175	10*	1,3
189	27	0,2
35	35	1
1	28	0

most theoretical and experimental attention of all dibaryons because it is expected to be the lightest [1]. This expectation follows from an  $O(\alpha_s)$  analysis of gluon-exchange diagrams.

How does one construct the state vector of the  $H$  dibaryon in terms of quark creation operators? Since each  $SU(3)$ -flavor representation appears just once in Table I, any six-quark configuration having relevant quantum numbers for a given dibaryon must be a valid state vector. It is useful to introduce a notation  $(abcdef)$  for spinless, colorless six-quark composites [5],

$$(abcdef) \equiv \epsilon^{\alpha\beta\gamma} \epsilon^{\eta\sigma\rho} \epsilon^{mn} \epsilon^{pq} \epsilon^{st} a_{\alpha m}^\dagger b_{\beta n}^\dagger c_{\gamma s}^\dagger d_{\eta p}^\dagger e_{\sigma q}^\dagger f_{\rho t}^\dagger |0\rangle, \quad (1)$$

where Greek indices run from 1 to 3 and denote color and Latin indices run from 1 to 2 and denote spin. The symbols  $\epsilon^{\alpha\beta\gamma}$  and  $\epsilon^{mn}$  are the usual antisymmetric tensors defined over the range of their indices. Under permutations of the labels, we have

$$(abcdef) = -(bacdef) = -(abcd ef). \quad (2)$$

A given dibaryon state vector will in general contain a linear combination of six-quark flavor components such as  $(abcdef)$ . The state vector of the  $H$  dibaryon can be found by constructing a singlet of flavor  $SU(3)$ . A linear combination which has this property is

$$|H\rangle = \frac{1}{144} [(udsuds) + (usdusd) + (dsudsu) - 2(ussudd) - 2(dssduu) - 2(usuds d)], \quad (3)$$

and so must be the  $H$ . This construction can then be employed in calculations of the mass and weak decay properties of the  $H$ .

The six-quark wave function is an object of some subtlety and can be subject to misinterpretation. For example, in the  $(abcdef)$  construction, the pairs  $a, b, d, e$ , and  $f$  have spin zero. It is possible to perform the spin coupling in an alternative manner, such that  $c$  and  $f$  still have spin zero, but  $a, b$  and  $d, e$  each couple to spin 1. The spin-1 pairs  $ab$  and  $de$  are then coupled to spin zero. This latter construction is denoted as

$$[abcdef] \equiv \epsilon^{\alpha\beta\gamma} \epsilon^{\eta\sigma\rho} \epsilon^{mn} a_{\alpha p}^\dagger (\sigma_i \sigma_2)_{pq} b_{\beta q}^\dagger c_{\gamma m}^\dagger d_{\eta r}^\dagger \times (\sigma_i \sigma_2)_{rs} e_{\sigma s}^\dagger f_{\rho n}^\dagger |0\rangle. \quad (4)$$

Expressed in terms of the  $[abcdef]$  structures, the  $H$  state vector has a very different appearance from Eq. (2). However, it can be shown [5] that the two  $H$  state vectors are identical since the absolute value of their inner product equals the product of their norms. It is also possible

to modify the way color is treated. In the color-singlet configurations corresponds to  $(abcdef)$  and  $[abcdef]$ , the triquarks  $abc$  and  $def$  are each color singlets. Alternatively, one can also obtain an overall color singlet from *color-octet*  $abc$  and  $def$  triquarks. Written this way, the resulting  $H$  state vector has yet a different appearance from the two mentioned above. However, as before, it can be shown to be identical to them. Such considerations imply that it is impossible to ascribe physical content to the spin and/or color coupling of the six quarks. All that counts is the overall singlet nature of the  $H$  as regards its spin, color, and flavor.

Recently, we have determined that additional conclusions can be reached. Observe that the quark representation of Eq. (3) contains six terms. It turns out that these do not form a linearly independent set because they exist in a vector space of dimension 4. To obtain this result requires performing calculations with six-quark state vectors. This is an exceedingly difficult process, and some matrix-element determinations would appear to be practically intractable. We have found that explicit calculations for the six-quark systems can be carried out successfully by combining analytic and numerical approaches. The latter method employs a pattern-recognition method which has become invaluable in probing properties of six-quark systems as well as higher-order contributions to arbitrary quark and gluon systems [6]. In an orthonormal basis obtained by diagonalizing the matrix displayed in Table II, the individual terms in Eq. (3) can be expressed as

$$\begin{aligned} (udsuds) &= 12\{-1, -\sqrt{1/3}, 1, \sqrt{5/3}\}, \\ (usdusd) &= 12\{1, -\sqrt{1/3}, 1, \sqrt{5/3}\}, \\ (dsudsu) &= 12\{0, \sqrt{4/3}, 1, \sqrt{5/3}\}, \\ (ussudd) &= 12\{0, -\sqrt{4/3}, 1, -\sqrt{5/3}\}, \\ (dssduu) &= 12\{-1, \sqrt{1/3}, 1, -\sqrt{5/3}\}, \\ (usuds d) &= 12\{1, \sqrt{1/3}, 1, -\sqrt{5/3}\}, \\ (sdusud) &= 12\{1, \sqrt{1/3}, 1/2, \sqrt{5/12}\}, \end{aligned} \quad (5)$$

with  $H$  having the decomposition

$$H = \{0, 0, -1/4, \sqrt{15}/4\}. \quad (6)$$

An alternative statement of the linear dependence is to note the relations obeyed by terms which appear in Eq. (3),

TABLE II. Six-quark overlap contributions.

	$(udsuds)$	$(usdusd)$	$(dsudsu)$	$(ussudd)$	$(dssduu)$	$(usuds d)$	$(sdusud)$
$(udsuds)$	576	288	288	0	0	-288	0
$(usdusd)$	288	576	288	0	-288	0	288
$(dsudsu)$	288	288	576	-288	0	0	288
$(ussudd)$	0	0	-288	576	288	288	-144
$(dssduu)$	0	-288	0	288	576	288	-144
$(usuds d)$	-288	0	0	288	288	576	144
$(sdusud)$	0	288	288	-144	-144	144	288

$$\begin{aligned} (usdusd) - (udsuds) + (dssduu) - (usudsd) &= 0, \\ (dsudsu) - (udsuds) + (ussudd) - (usudsd) &= 0. \end{aligned} \quad (7)$$

These relations can be used to eliminate two of the terms in Eq. (3) and thus express  $H$  in terms of the nonorthogonal basis provided by just four of the six-quark composites.

### B. Possibility of a baryon-baryon representation

A final question regarding the  $H$  state vector remains: Is it meaningful to express  $H$  explicitly in terms of *baryon-baryon* states? Equation (3) describes the  $H$  in terms of quark degrees of freedom—the hadronic content is far from evident. One is motivated to attempt the following construction. Imagine two baryons confined within a bag. In order to be constituents of the  $H$ , they would be required to have a total spin equal to zero. We shall denote such a hypothetical configuration with quotations, viz.,  $|\text{“}B_1 B_2\text{”}\rangle$ .

We shall use several arguments to show that it is not meaningful to express the six-quark state vector of the  $H$  into such  $|\text{“}B_1 B_2\text{”}\rangle$  components. In fact, the very name “ $H$  dibaryon” is unfortunate because it misleadingly suggests that the six quarks (i.e., two each of  $u, d, s$ ) can be associated with two baryons in some distinct manner. Insofar as the six quarks have similar spatial wave functions, there can be no such identification.

To begin, let us study the bag-enclosed six-quark configuration  $|\text{“}\Lambda\Lambda\text{”}\rangle$  whose state vector is that of two  $\Lambda(1116)$  baryons in a state of total spin  $S=0$ . Recall that the quark-model state vector for a single  $\Lambda(1116)$  of spin component  $k$  is

$$\begin{aligned} |\Lambda_k\rangle &= \epsilon^{\alpha\beta\gamma} \frac{1}{\sqrt{12}} [u_{\alpha\uparrow}^\dagger d_{\beta\downarrow}^\dagger - u_{\alpha\downarrow}^\dagger d_{\beta\uparrow}^\dagger] s_{\gamma k}^\dagger |0\rangle \\ &= \frac{\epsilon^{\alpha\beta\gamma} \epsilon^{mn}}{\sqrt{12}} u_{\alpha m}^\dagger d_{\beta n}^\dagger s_{\gamma k}^\dagger |0\rangle. \end{aligned} \quad (8)$$

The normalization factor  $(12)^{-1/2}$  simply counts the possible color-spin configurations which the three quarks can occupy—there are six color configurations in which the  $u$  quark has spin up and six in which the  $u$  quark has spin down.

It is possible to express the state vector  $|\text{“}\Lambda\Lambda\text{”}\rangle$  in the notation of Eq. (1),

$$|\text{“}\Lambda\Lambda\text{”}\rangle = \frac{1}{N_{\Lambda\Lambda}} (udsuds), \quad (9)$$

where  $N_{\Lambda\Lambda}$  is a normalization factor. The above construction suggests that each of the terms in Eq. (3) might have an analogous interpretation as a spinless baryon-baryon pair. However, this is not the case. For example, a naive argument for determining the normalization  $N_{\Lambda\Lambda}$  would suggest that

$$N_{\Lambda\Lambda}^{(\text{naive})} = 12\sqrt{2}, \quad (10)$$

with the 12 arising from multiplying the individual  $\sqrt{12}$  factors in the two  $\Lambda$  state vectors and the extra  $\sqrt{2}$  factor being the SU(2) Clebsch-Gordon coefficients for combining two spin- $\frac{1}{2}$  entities to form a system of spin zero.

However, such reasoning cannot replace a real calculation and indeed gives the wrong answer. Calculation of  $N_{\Lambda\Lambda}$  reveals the correct value to be

$$N_{\Lambda\Lambda} = 24. \quad (11)$$

Thus the normalization factor which appears in Eq. (9) is not the result of simply squaring the normalization in Eq. (4) and including the effect of spin coupling. A physical explanation for this resides in Fig. 1, which depicts typical diagrams which contribute to the normalization condition  $\langle \text{“}\Lambda\Lambda\text{”} | \text{“}\Lambda\Lambda\text{”} \rangle = 1$ . Observe that a quark of a given flavor can be contracted in more than one way, as in Fig. 1. The presence of such interfering amplitudes means that the unit-normalized  $|\text{“}\Lambda\Lambda\text{”}\rangle$  state is not a pair of  $\Lambda(1116)$  baryons occupying some baglike region of space. Instead, it is just a six-quark configuration in which the colors, spins, and flavors are coupled to give a set of prescribed quantum numbers, in this case  $B=2$ ,  $Y=0$ , and  $S=I=0$ . This simple example reveals the impossibility of associating the six bound quarks in a unique manner with particular hadrons. Only if the quarks were physically separated into two three-quark clusters (as in the case of the deuteron) would it make sense to imply such an identification, since the interference between the different clusters would then be greatly suppressed.

For another example leading to the same conclusion, let us return to the issue of interpreting the terms in Eq. (3) as baryon-baryon states. Writing the  $\Sigma^0$  state vector corresponding to spin component  $k$  as

$$|\Sigma_k^0\rangle = \frac{\epsilon^{\alpha\beta\gamma} \epsilon^{mn}}{6} (s_{\alpha m}^\dagger d_{\beta n}^\dagger u_{\gamma k}^\dagger + s_{\alpha m}^\dagger u_{\beta n}^\dagger d_{\gamma k}^\dagger) |0\rangle,$$

it is easy to construct the spinless two- $\Sigma^0$  state, and one finds

$$\begin{aligned} |\text{“}\Sigma^0 \Sigma^0\text{”}\rangle &= -\frac{1}{36\sqrt{2}} [(sdusdu) + (sudsud) \\ &\quad + 2(sdusud)]. \end{aligned} \quad (12)$$

However, in view of the linear dependence exhibited by the six-quark states, one can express this combination in terms of other of the  $|\text{“}B_1 B_2\text{”}\rangle$  states,

$$\begin{aligned} |\text{“}\Sigma^0 \Sigma^0\text{”}\rangle &= [-|\text{“}\Lambda\Lambda\text{”}\rangle + |\text{“}n\Xi^0\text{”}\rangle + |\text{“}p\Xi^-\text{”}\rangle \\ &\quad - 2|\text{“}\Sigma^+ \Sigma^-\text{”}\rangle]. \end{aligned} \quad (14)$$

Thus any construction based on the  $|\text{“}B_1 B_2\text{”}\rangle$  construction would not be unique.

Accepting that the  $H$  state vector cannot support a simple baryon-baryon representation, one is still left with the following question. Since  $H$  transforms as a singlet under flavor SU(3), we know that it must couple to physi-

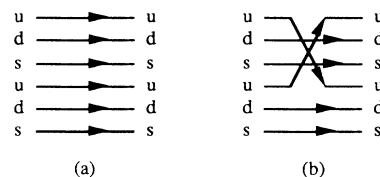


FIG. 1. Two examples of six-quark contractions.

cal two-baryon flavor channels with probabilities  $P_{B_1 B_2}$  given by

$$P_{\Lambda^0 \Lambda^0} = P_{\Sigma^0 \Sigma^0} = \frac{1}{8}, \quad P_{p \Xi^-} = P_{n \Xi^0} = P_{\Sigma^+ \Sigma^-} = \frac{2}{8}, \quad (15)$$

or equivalently in terms of isospin states,

$$P_{\Lambda \Lambda} = \frac{1}{8}, \quad P_{\Sigma \Sigma} = \frac{3}{8}, \quad P_{N \Xi} = \frac{4}{8}. \quad (16)$$

Physically, these relations mean that if the  $H$  could decay to all the two-baryon channels, then a detector in a given hemisphere would have four ways to infer the presence of the  $N \Xi$  mode ( $p, n, \Xi^0, \Xi^-$ ), three for the  $\Sigma \Sigma$  mode ( $\Sigma^+, \Sigma^0, \Sigma^-$ ), and just one for the  $\Lambda \Lambda$  mode.

We have found that interference effects among the quarks in a six-particle composite precludes any interpretation of the  $H$  state vector in terms of baryon pairs. However, should not one be able, at least in principle, to extract the hadronic couplings of the  $H$  from Eq. (3)? Here is a simple procedure for doing this: (i) Write the various (unconfined) final-state spin-zero two-baryon states (denoted as  $|B_1 B_2\rangle$ ) in quark notation but use a normalization appropriate for noninterfering baryons, and then (ii) actually perform the overlaps of such state vectors with that of the  $H$ . The physical picture of the state  $|B_1 B_2\rangle$  is that of two physically distinct baryons which propagate with opposite momenta in the  $H$  rest frame. In principle, such overlaps will each be proportional to a factor which depends on the individual spatial wave functions and which determines the overall scale of the coupling. A simple calculation recovers the SU(3)-flavor dependence given in Eqs. (15) and (16).

### III. DIQUARKS

Only color-singlet configurations have been found in nature. On the other hand, diquarks must be assigned to either of the color representations  $\mathbf{6}$  or  $\mathbf{3}^*$ . Since such color-bearing configurations cannot propagate in the physical vacuum, it would appear that diquarks are of little interest. However, it has proved profitable to study the properties of such objects, and there already exists a substantial literature relating to them. It is impossible to list all the references here, but a few examples might suffice. For instance, there has been recent work [7] on the possible existence of a “diquark phase” in quark matter which is in a state of thermodynamic equilibrium. Diquarks have also been used to model a possible dynamical pairing between quarks as they move within baryons [8]. Such clustering would affect the values of physical observables and thus modify quark-model predictions [8,9]. Also, the diquark picture has been invoked to describe possible effects in scattering reactions [10]. However, the opinion on diquarks is not uniformly positive [11]. As with most topics in QCD, there is clearly much work left to be done.

Let us enumerate the possible diquark configurations. The diquark state vector has flavor, spin, and color degrees of freedom. The key constraint is that of Fermi

TABLE III. Allowable diquark configurations.

Flavor	Spin	Color
$\mathbf{3}^*$	0	$\mathbf{3}^*$
$\mathbf{3}^*$	1	$\mathbf{6}$
$\mathbf{6}$	0	$\mathbf{6}$
$\mathbf{6}$	1	$\mathbf{3}^*$

statistics—such state vectors must be antisymmetric under interchange of the two quarks. We shall be working with the SU(3) of flavor and so shall consider the diquark configurations displayed in Table III. Observe that there are four allowed configurations. We shall employ the notation  $|\mathbf{F}, \mathbf{S}, \mathbf{C}\rangle_\sigma^{m_S}$  for the associated state vectors, where  $\mathbf{F}$ ,  $\mathbf{S}$ ,  $\mathbf{C}$ , and  $m_S$  represent flavor, total spin, color, and spin component, respectively, and  $\sigma$  denotes a particular member of the multiplet. In terms of quark creation operators, the corresponding Fock-space representations are given for members of the diquark multiplets by

$$\begin{aligned} |3^*, 0, 3^*\rangle_{ud}^0 &= \frac{1}{2} \epsilon^{\alpha\beta\gamma} \epsilon^{mn} u_\alpha^\dagger d_\beta^\dagger |0\rangle, \\ |3^*, 1, 6\rangle_{ud}^1 &= u_\uparrow^\dagger d_\uparrow^\dagger |0\rangle, \\ |6, 0, 6\rangle_{uu}^0 &= u_\uparrow^\dagger u_\downarrow^\dagger |0\rangle, \\ |6, 1, 3^*\rangle_{uu}^1 &= \frac{1}{2} \epsilon^{\alpha\beta\gamma} u_\alpha^\dagger u_\beta^\dagger |0\rangle, \\ &\vdots \end{aligned} \quad (17)$$

State vectors such as these will form the foundation for our analysis, as described in the following section.

### IV. CALCULATING HIGHER-ORDER PERTURBATIONS

#### A. Formalism

While the bag model itself can be cast in a relativistically covariant manner, the static-cavity approximation cannot. Thus we do not employ covariant perturbation theory, but refer instead to the noncovariant approach developed first in nonrelativistic many-body theory. The key theorem is that of Gell-Mann and Low, which is used to find eigenstates of the Hamiltonian  $H = H_0 + H_1$  in the basis of eigenstates  $\{|\Phi_\alpha\rangle\}$  of the unperturbed Hamiltonian  $H_0$ ,

$$H_0 |\Phi_\alpha\rangle = E_0 |\Phi_\alpha\rangle. \quad (18)$$

In particular, the ground state  $|\Phi_0\rangle$  is allowed to evolve adiabatically from  $t = -\infty$  to 0 under the influence of Hamiltonian  $H_\epsilon$ ,

$$H_\epsilon = H_0 + e^{\epsilon|t|} H_1. \quad (19)$$

The evolution of  $|\Phi_0\rangle$  under the adiabatic switching on of  $H_1$  is described by the time-evolution operator  $U_\epsilon(0, -\infty)$  [12],

$$U_\epsilon(0, -\infty) = \sum_{k=0}^{\infty} \frac{(-i)^k}{k!} \int_{-\infty}^0 dt_1 \cdots \int_{-\infty}^0 dt_k e^{\epsilon(t_1 + \cdots + t_k)} T[H_1(t_1) \cdots H_k(t_k)]. \quad (20)$$

The theorem of Gell-Mann and Low addresses the fact that the phase of the state  $U_\epsilon(0, -\infty)|\Phi_0\rangle$  diverges in the  $\epsilon \rightarrow 0$  limit. For our purpose the result of most significance is the energy-shift formula

$$\Delta E \equiv E - E_0 = \frac{\langle \Phi_0 | H_1 | \Psi_0 \rangle}{\langle \Phi_0 | \Psi_0 \rangle} = \lim_{\epsilon \rightarrow 0} \frac{N}{D}, \quad (21)$$

where we define both the numerator function  $N$ ,

$$N \equiv \langle \Phi_0 | H_1 U_\epsilon(0, -\infty) | \Phi_0 \rangle, \quad (22)$$

and the denominator function  $D$ ,

$$D \equiv \langle \Phi_0 | U_\epsilon(0, -\infty) | \Phi_0 \rangle. \quad (23)$$

A compact expression due to Goldstone [13] for computing  $\Delta E$  is given by

$$\Delta E = \left\langle \Phi_0 \left| H_1 \sum_{k=0}^{\infty} [(E_0 - H_0)^{-1} H_1]^k \right| \Phi_0 \right\rangle_c, \quad (24)$$

where the subscript  $c$  stands for ‘‘connected.’’ This formula holds only when the state  $|\Phi_0\rangle$  is a zero-particle state. It has application to many-body theory when the ground state can be written as a filled Fermi sea, as is the case for some nuclei. In this circumstance the interactions create particle-hole pairs.

We shall be studying systems for which the initial and final states,  $|\Phi_0\rangle$  and  $\langle \Phi_0|$  generally have non-zero-particle number. As before, it is important to work with quantities which remain finite as the interaction is turned on and then off. It can be shown [6] that the decomposition of Eq. (21) still holds, but now with the numerator function

$$N = N_c^f D \quad (25)$$

and energy shift

$$\Delta E = \lim_{\epsilon \rightarrow 0} N_c^f. \quad (26)$$

To express the energy shift in a Goldstone-like form such as that of Eq. (24), we display the time dependence of the interaction  $H_1$  in the interaction picture,

$$H_1(t_1) = e^{iH_0 t_1} H_1 e^{-iH_0 t_1}, \quad (27)$$

to obtain

$$\begin{aligned} \Delta E = \lim_{\epsilon \rightarrow 0} \sum_{k=0}^{\infty} \langle \Phi_0 | H_1 (E_0 - H_0 + ki\epsilon)^{-1} \\ \times H_1 [E_0 - H_0 + (k-1)i\epsilon]^{-1} \\ \times \cdots [E_0 - H_0 + i\epsilon]^{-1} H_1 | \Phi_0 \rangle_c^f. \end{aligned} \quad (28)$$

The final result may be expressed as

$$\Delta E = \left\langle \Phi_0 \left| H_1 \sum_{k=0}^{\infty} [(E_0 - H_0)^{-1} H_1]^k \right| \Phi_0 \right\rangle_c^f. \quad (29)$$

Some thought must be given to connected diagrams for which  $|\Phi_0\rangle$  appears as an intermediate state in Eq. (28)

and thus may formally diverge in the  $\epsilon \rightarrow 0$  limit. The superscript  $f$  denotes the ‘‘finite’’ part of such naively divergent contribution. The derivation of this result is long and involved [6]. We shall present only a prescription for evaluating the finite part of a naively divergent quantity.

To evaluate Eq. (28), one inserts complete sets of the unperturbed eigenstates between the various  $(E_0 - H_0)^{-1} H_1$  factors and obtains, in the  $\epsilon = 0$  limit,

$$\begin{aligned} \sum_{n_1, \dots, n_k} \langle \Phi_0 | H_1 | n_1 \rangle \langle n_1 | (E_0 - H_0)^{-1} H_1 | n_2 \rangle \\ \times \langle n_2 | \cdots | n_k \rangle \langle n_k | (E_0 - H_0)^{-1} H_1 | \Phi_0 \rangle_c. \end{aligned} \quad (30)$$

The adjacent intermediate state is used to evaluate each of the  $H_0$  operators. However, if  $|\Phi_0\rangle$  is the intermediate state in question, then  $E_0 - H_0 = 0$ . Thus  $(E_0 - H_0)^{-1}$  leads to a divergence, and so an appropriately defined finite part must be used instead. The procedure indicated by the finite part may be summarized as follows: *In a diagram having the intermediate states  $n_1, \dots, n_k$  [with indices ordered as in Eq. (30)], any factor  $\langle n_i | (E_0 - H_0 + i\epsilon)^{-1}$  which diverges as  $\epsilon \rightarrow 0$  should be replaced by the quantity  $-\sum_{j=1}^{i-1} \langle n_j | (E_0 - H_0 + i\epsilon)^{-1}$ .* This procedure has been checked with a number of soluble examples, one of which is considered in the Appendix for the purpose of illustration.

## B. Truncated bag model

For definiteness, the bag model is used to supply quark and gluon spatial wave functions throughout the calculation. Specifically, we work in the ‘‘truncation approximation’’ in which only the lowest bag mode is taken into account. This has proved to be the most important contribution in previous applications of the bag model and should supply a reasonable estimate of the effects we study in this paper. The chief motivation for employing such an approximation is that it enables one to perform a systematic investigation of higher-order perturbative terms [6]. For complicated calculations, such as those which occur in computing radiative corrections for six-quark states, a truncationlike approximation is clearly warranted. Interestingly, it is the analytic counterpart of the so-called ‘‘quenched’’ approximation used in lattice gauge theory—in both approaches, quark-antiquark loops are absent.

To complete this section, we list the types of interactions which are included in the perturbative Hamiltonian  $H_1$ . First, there are the interactions of dynamic gluons. These are described in the truncation approximation by the *quark-gluon* vertex

$$\frac{\sqrt{\alpha_s}}{R} M(mR) \sigma_{\mu\nu}^i \lambda_{ab}^A \quad (31)$$

and the *three-gluon* vertex

$$-\frac{\sqrt{\alpha_s}}{R} P \epsilon^{ijk} f^{ABC}. \quad (32)$$

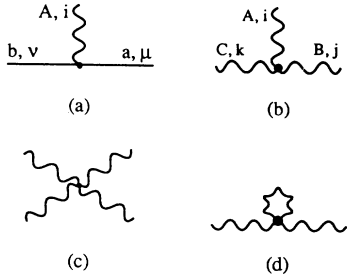


FIG. 2. Non-Coulombic QCD vertices.

In the above the bag radius is denoted as  $R$ , and we employ the quark mass value  $m_{u,d}=0$ , but study the effect of varying the strange-quark mass  $m_s$ . The *four-gluon* vertex of Fig. 2(c) will not be needed in our  $O(\alpha_s^2)$  analysis since we would require the gluon legs to hook onto quark lines, thus implying an  $O(\alpha_s^3)$  contribution [14]. The forms of these vertices correspond to the notation appearing in Fig. 2. The quantities  $M$  and  $P$  are quark and/or gluon overlap integrals and are given by

$$M(mR) = \left[ \frac{2}{3} \right]^{1/2} \bar{N}_G \bar{N}_Q^2(mR) \frac{P}{\omega + mR} \times \int_0^1 du u^2 j_0(pu) j_1(pu) j_1(ku), \quad (33)$$

$$P = 3 \left[ \frac{3}{2} \right]^{1/2} \bar{N}_G^3 \int_0^1 du u j_1^3(ku) \simeq 0.680,$$

where  $M(0) \simeq 0.246$  and reduced quark and gluon normalization factors are denoted as  $\bar{N}_G \equiv RN_G$  and  $\bar{N}_Q \equiv R^{3/2} N_Q$ , respectively.

### C. Calculations

#### 1. Diquarks

Using the formalism described above, we have considered the effect of  $O(\alpha_s^2)$  corrections upon the diquark systems identified in Sec. III. Of course, since diquarks are nonphysical entities, there is a question of how to proceed. In principle, diquarks can exist in a variety of distinct environments, such as a quark-gluon plasma or as a component of a single baryon. Here we do not wish to consider any specific environment, and so we do not perform a computation of “absolute” diquark masses. Rather, we explore the question of relative binding, extending in the most natural possible manner previous analyses of the  $O(\alpha_s)$  exchange diagrams. Thus we have chosen to compute the diquark diagrams shown in Fig. 3, ignoring both quark self-energy and Coulomb effects. Since diquarks are not physical color-singlet objects, their environment must be considered for a proper determination of Coulomb effects. Quark self-energies are omitted because they do not affect binding.

Our findings are naturally expressed as the following expansion in  $\alpha_s$ :

$$\begin{aligned} \Delta E(3^*, 0, 3^*) &= -0.35 \frac{\alpha_s}{R} - 0.21 \frac{\alpha_s^2}{R}, \\ \Delta E(3^*, 1, 6) &= -0.06 \frac{\alpha_s}{R} - 0.06 \frac{\alpha_s^2}{R}, \\ \Delta E(6, 0, 6) &= 0.18 \frac{\alpha_s}{R} + 0.14 \frac{\alpha_s^2}{R}, \\ \Delta E(6, 1, 3^*) &= 0.12 \frac{\alpha_s}{R} + 0.10 \frac{\alpha_s^2}{R}. \end{aligned} \quad (34)$$

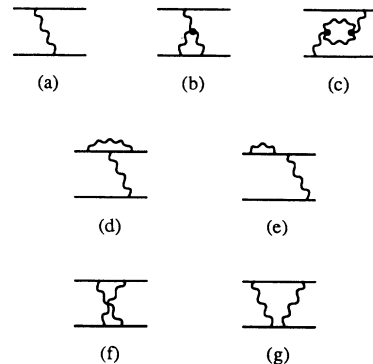
The numerical values which appear as coefficients in the above expansions are composed of quark and gluon normalization and wave-function-overlap factors, as described earlier [15]. Let us defer further comment on these results to the summary in Sec. V and instead move on to a discussion of higher-order contributions to the  $H$ -dibaryon mass.

#### 2. $H$ dibaryon

The diagrams on which our calculation of the  $H$  mass is based are shown in Figs.3–5. These incorporate processes involving both dynamic-gluon degrees of freedom and color-Coulombic effects. For completeness, we display in Fig. 6 higher-order diagrams which one might have expected to contribute, but which in fact can be shown to vanish. In order to obtain the  $H$  mass in absolute terms, specific values for the phenomenological parameters which appear in the bag model are required. We have performed a careful  $O(\alpha_s^2)$  analysis of the observed baryon and meson ground-state spectrum to fix these quantities, resulting in

$$\begin{aligned} B^{1/4} &= 0.167 \text{ GeV}, \\ Z_0 &= -0.97, \\ \alpha_s &= 0.84, \\ m_s &= 0.244 \text{ GeV}. \end{aligned} \quad (35)$$

The above value for  $\alpha_s$  is noteworthy because it is so small compared to the usual value ( $\alpha_s = 2.2$ ) typically cited in the literature. Our reduced value is a direct consequence of the higher-order nature of our calculation. Recall that the main determining factor of  $\alpha_s$  is the  $\Delta$ - $N$

FIG. 3. Two-quark  $O(\alpha_s^2)$  non-Coulombic QCD interactions.

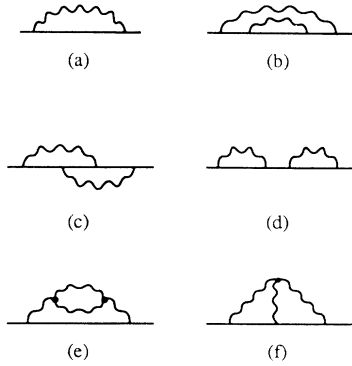


FIG. 4. Quark  $O(\alpha_s^2)$  non-Coulombic QCD self energies.

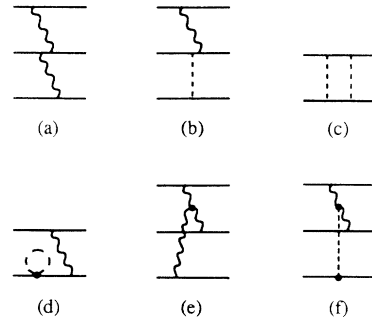


FIG. 6. Diagrams contributing zero to the  $H$ -dibaryon mass.

mass difference. At the level of a first-order analysis, the burden of reproducing the experimental mass splitting resides in  $\alpha_s$  itself. However, higher-order gluon effects tend to reinforce the effect of the lowest-order gluon-exchange contribution. Indeed, some (but not all) of the  $O(\alpha_s^2)$  gluon-exchange graphs have the same “color-color”  $\times$  “spin-spin” structure as single-gluon exchange. The end result of having a number of diagrams which produce the same overall effect is to lessen the need for  $\alpha_s$  to be so large.

Using the (truncated) bag-model parameters of Eq. (35), we have computed the mass  $M_H$ . Various classes of contributions are given in Table IV. An instructive manner of displaying the results is to list the mass for calculations (with fixed input parameters) performed sequentially at  $O(\alpha_s^0)$  next at  $O(\alpha_s^1)$ , and then at  $O(\alpha_s^2)$ . Remembering that the bag-model equations provide a value for the bag radius  $R$  as well as the mass, we have

$$\begin{aligned}
 M_H &= 2.84 \text{ GeV}, \quad R = 5.88 \text{ GeV}^{-1} [O(\alpha_s^0)], \\
 M_H &= 2.39 \text{ GeV}, \quad R = 5.52 \text{ GeV}^{-1} [O(\alpha_s^1)], \\
 M_H &= 2.19 \text{ GeV}, \quad R = 5.35 \text{ GeV}^{-1} [O(\alpha_s^2)].
 \end{aligned}
 \tag{36}$$

Finally, the effect of separately varying  $m_s$  and  $\alpha_s$  is shown, respectively, in Figs. 7 and 8. Each figure con-

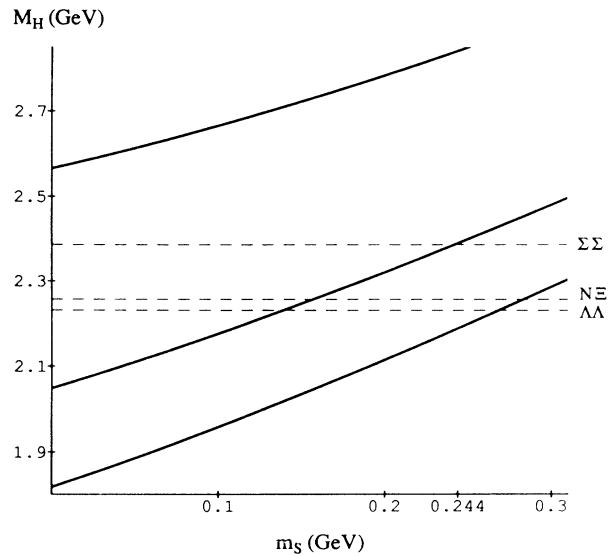


FIG. 7. Dependence of  $H$  mass on strange-quark mass ( $m_s = 0.244 \text{ GeV}$  represents the actual prediction).

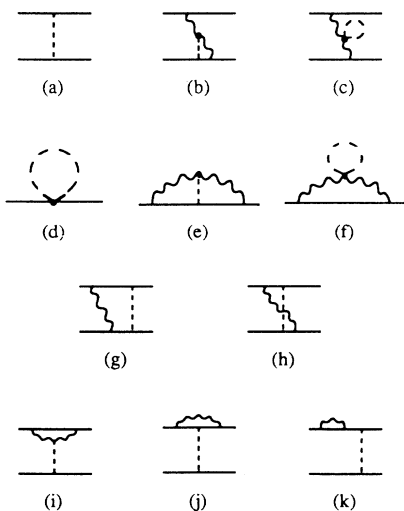


FIG. 5.  $O(\alpha_s^2)$  QCD Coulombic interactions.

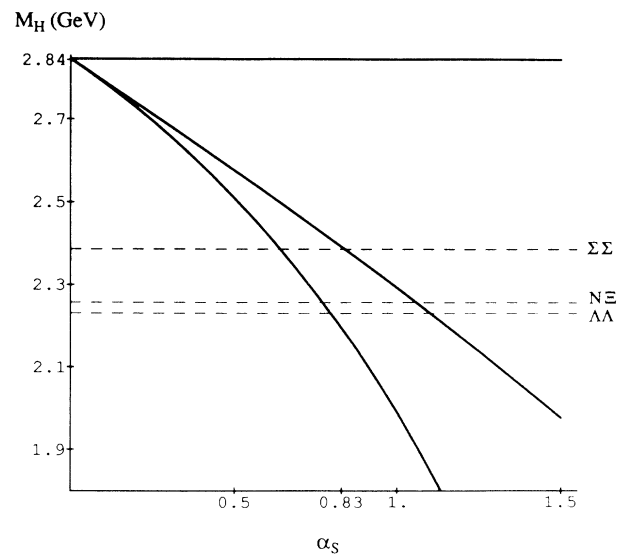


FIG. 8. Dependence of  $H$  mass on  $\alpha_s$  ( $\alpha_s = 0.84$  represents the actual prediction). The horizontal curve at the top corresponds to the  $O(\alpha_s^0)$  calculation.

TABLE IV. Contributions to the mass of the  $H$ .

$m_s R$	0	1	2
	12.26	13.36	14.73
Kinetic energy	$\frac{R}{1.06\alpha_s} - \frac{0.56\alpha_s^2}{R}$	$\frac{R}{0.96\alpha_s} - \frac{0.51\alpha_s^2}{R}$	$\frac{R}{0.85\alpha_s} - \frac{0.45\alpha_s^2}{R}$
Dynamic gluon	$\frac{R}{2.12\alpha_s} - \frac{R}{1.03\alpha_s^2}$	$\frac{R}{1.93\alpha_s} - \frac{R}{0.93\alpha_s^2}$	$\frac{R}{1.78\alpha_s} - \frac{R}{0.86\alpha_s^2}$
Quark self-energy	$\frac{R}{0.04\alpha_s^2} - \frac{R}{R}$	$\frac{R}{0.01\alpha_s} - \frac{R}{0.05\alpha_s^2}$	$\frac{R}{0.03\alpha_s} - \frac{R}{0.06\alpha_s^2}$
Coulomb	$\frac{R}{R}$	$\frac{R}{R} + \frac{R}{R}$	$\frac{R}{R} + \frac{R}{R}$

tains three curves, which correspond from top to bottom to the respective cases  $O(\alpha_s^0)$ ,  $O(\alpha_s^1)$ , and  $O(\alpha_s^2)$  [16]. As one would expect,  $M_H$  increases with  $m_s$  since strange quarks represent two of the six constituents and decreases with  $\alpha_s$  since the overall effect of gluon dynamics is to bind the  $H$ . In these figures we also display the  $\Lambda\Lambda$ ,  $N\Xi$ , and  $\Sigma\Sigma$  thresholds as an aid in determining the conditions under which the  $H$  is either stable or unstable.

## V. CONCLUDING REMARKS

As mentioned in the Introduction, previous insights regarding the dynamical behavior of diquarks and dibaryons have largely been inferred from calculations which are of first order in the strong interactions. While useful enough to serve as the basis for inferences regarding these systems, such studies are subject to the criticism that they may be unstable with respect to the inclusion of higher orders. Unfortunately, work on higher-order effects has been hindered by the extraordinary calculational difficulty of dealing with six-quark state vectors. Our ability to overcome this has allowed the studies described in earlier pages.

An instructive analogy involving second-order corrections occurs with attempts to compute the spectrum of  $0^{++}$  glueballs. In the bag model, the lowest-order mass estimate consists mainly of the energy of a pair of constituent gluons and yields a value above 1 GeV. Further calculation reveals that the  $O(\alpha_s)$  corrections are large and negative, driving the total mass to zero or even to negative values (depending on the precise values of the bag parameters). However, the  $O(\alpha_s^2)$  contributions turn out to upset the  $O(\alpha_s)$  effects and to restore the mass estimate to a value in excess of 1 GeV [6]. Interestingly, this is in accord with results of quenched lattice gauge computations [17] (which the truncation approach indeed mimics).

In the case of the  $H$  dibaryon, we have carried out our studies under a variety of conditions, such as differing input parameters and differing treatments of center-of-mass effects. For example, we find that (i) allowing the non-strange quarks to have nonzero mass has negligible effect on the  $H$  mass, (ii) omitting the center-of-mass motion correction (and thereby modifying the value of  $Z_0$ ) somewhat lowers the  $H$  mass, (iii) omitting the Coulomb interaction and redoing the overall fit lowers the  $H$  mass even more, etc. We have found the values for the  $H$  mass

thus obtained to fall in the range  $2.12 < M_H$  (GeV)  $< 2.19$ . The central value  $M_H = 2.15$  GeV would imply an  $H$  which is stable against strong decay, lying roughly 80 MeV below the  $\Lambda\Lambda$  threshold. Although one could cite a lattice study [18] which yields similar results, it would be premature to claim that a stable  $H$  must exist. Neither model nor existing lattice calculations can claim to be rigorous reflections of the dynamics of color. However, a calculation such as ours supports the experimental search for the  $H$  [19], and we would urge such efforts to continue.

Although the enterprise described here has entailed considerable effort, further work comes to mind. It seems to us that the following topics deserve special attention.

(i) The most obvious extension of our calculation regards relaxation of the truncation approximation. Experience with studies of mesons and baryons suggests that the influence of the lowest-energy negative-parity bag contribution is the next most important mode to consider. It should be understood, however, that this will greatly increase the number of diagrams, as quark-antiquark loops must then be taken into account.

(ii) The somewhat more formal question of gauge invariance also deserves attention. The point is whether the dynamical assumption of "truncation," carried out to an arbitrary order of perturbation theory, is or is not gauge invariant. Our own calculation, albeit done carefully, is carried out within a given gauge and does not address this more general issue. Although it is reassuring that an  $O(\alpha_s)$  calculation of meson and baryon properties which also incorporates the use of truncation is evidently gauge invariant [20], this by itself is also not sufficient to settle the matter to higher orders.

(iii) Another subject of potential importance is that of determining the modification to the  $H$  state vector induced by mixing with baryon-baryon continuum states. The analysis carried out here clearly does not take this possibility into account. It is not easy for us to quantitatively estimate whether this effect is more important than others, say, point (i) above. However, it is one which properly belongs on the list of future efforts.

Finally, our main result for diquark systems appears in Eq. (34), which displays the  $O(\alpha_s^2)$  energy contribution for each of the four allowed diquarks. Our conclusion is that the binding of the  $(3^*, 0, 3^*)$  is indeed the deepest of the diquarks and that the only other configuration which



shows any tendency to bind is the  $(3^*, 1, 6)$ . Thus our work reinforces the first-order analysis and should be regarded as support for serious attempts (e.g., Ref. [21]) to infer physical consequences of dynamically bound (or at least highly correlated) diquarks.

#### ACKNOWLEDGMENTS

The research described in this paper was supported in part by the National Science Foundation. One of us (E.G.) wishes to acknowledge the kind hospitality of the theory group at the Rutherford Appleton Laboratory, where part of the work described herein was performed.

#### APPENDIX:

##### EXAMPLE OF A FINITE CONTRIBUTION

In the appendix we shall demonstrate the calculational procedure introduced in Sec. IV A by means of a simple example containing a fermion field and a boson field. The fermionic quanta are allowed to occupy either of two degenerate states of energy  $\omega$  and have destruction operators  $b_i (i=1,2)$ . The bosonic quanta can occupy any of three degenerate states of energy  $k$  and have destruction operators  $a_m (m=1,2,3)$ . The interaction of these quanta is governed by

$$V = gb^\dagger \sigma^m b (a_m^\dagger + a_m), \quad (\text{A1})$$

where  $\sigma^m$  is a Pauli matrix,  $g$  is a coupling constant, and there are implicit sums over index  $m$  as well as suppressed fermion indices. In the following we shall determine the energy of a one-fermion state through fourth order in the interaction. For purposes of comparison, we shall perform the calculation in two ways: first with the ordinary Rayleigh-Schrödinger approach and then with our equivalent technique (cf. Sec. IV A).

We begin by recalling the standard formulas of Rayleigh-Schrödinger perturbation theory. The Hamiltonian is written  $H = H_0 + \lambda V$ , where the eigensolutions of the unperturbed Hamiltonian  $H_0$  are

$$H_0 |\phi_\alpha\rangle = E_\alpha^{(0)} |\phi_\alpha\rangle. \quad (\text{A2})$$

We denote the ground state of the full Hamiltonian by  $|\psi\rangle$  having energy  $E$ ,

$$(H_0 + \lambda V) |\psi\rangle = E |\psi\rangle. \quad (\text{A3})$$

The perturbative relations of interest to us here are

$$E = E_0^{(0)} + \lambda E_0^{(1)} + \lambda^2 E_0^{(2)} + \dots \quad (\text{A4})$$

and

$$|\psi\rangle = |\phi_0\rangle + \lambda |\psi_1\rangle + \lambda^2 |\psi_2\rangle + \dots, \quad (\text{A5})$$

where

$$|\psi_1\rangle = \sum_\alpha c_\alpha^{(1)} |\phi_\alpha\rangle, \quad |\psi_2\rangle = \sum_\alpha c_\alpha^{(2)} |\phi_\alpha\rangle. \quad (\text{A6})$$

The (well-known) expressions for the first four energy perturbations are just

$$\begin{aligned} E_0^{(1)} &= \langle \phi_0 | V | \phi_0 \rangle, \\ E_0^{(2)} &= - \sum_{\alpha \neq 0} \frac{\langle \phi_0 | V | \phi_\alpha \rangle \langle \phi_\alpha | V | \phi_0 \rangle}{E_\alpha - E_0}, \\ E_0^{(3)} &= \sum_{\alpha \neq 0} \frac{\langle \phi_0 | V | \phi_\alpha \rangle}{E_\alpha - E_0} X_\alpha, \\ E_0^{(4)} &= - \sum_{\alpha \neq 0} \frac{\langle \phi_0 | V | \phi_\alpha \rangle}{E_\alpha - E_0} \left[ \sum_{\beta \neq 0} \frac{\langle \phi_0 | V | \phi_\beta \rangle}{E_\beta - E_0} X_\beta \right. \\ &\quad \left. + E^{(1)} X_\alpha + E_0^{(2)} \frac{\langle \phi_\alpha | V | \phi_0 \rangle}{E_\alpha - E_0} \right], \end{aligned} \quad (\text{A7})$$

where

$$X_\alpha = - \sum_{\beta \neq 0} \frac{\langle \phi_\alpha | V | \phi_\beta \rangle \langle \phi_\beta | V | \phi_0 \rangle}{E_\beta - E_0} - \frac{\langle \phi_\alpha | V | \phi_0 \rangle E^{(1)}}{E_\alpha - E_0}. \quad (\text{A8})$$

Since it is straightforward to calculate these energies, we shall omit all details and proceed directly to the results:

$$\begin{aligned} E_0^{(1)} &= 0, \\ E_0^{(2)} &= - \frac{3g^2}{k}, \\ E_0^{(3)} &= 0, \\ E_0^{(4)} &= \frac{6g^4}{k^3}. \end{aligned} \quad (\text{A9})$$

Alternatively, we can do the calculation using our diagrammatic approach. It is easy to see that the first- and third-order contributions must vanish. The diagrams for the second- and fourth-order energy shifts are precisely the same as in Figs. 4(a)–4(d). The second-order energy contribution, which has no potentially divergent parts, is given by

$$\begin{aligned} \Delta^{(2)} &= \langle \phi_0 | V (E_0 - H_0)^{-1} V | \phi_0 \rangle \\ &= g^2 \left\langle \phi_0 \left| \frac{\sigma^m \sigma^m}{\omega - (\omega + k)} \right| \phi_0 \right\rangle = - \frac{3g^2}{k}. \end{aligned} \quad (\text{A10})$$

Of more interest are the three fourth-order diagrams, [Figs. 4(b)–4(d)]. The last of these is the only one from which we must extract a “finite part.” The associated energy contributions are, respectively,

$$\begin{aligned} \Delta E_0^{(4)b} &= g^4 \left\langle \phi_0 \left| \sigma^m \frac{-1}{k} \sigma^n \frac{-1}{2k} \sigma^n \frac{-1}{k} \sigma^m \right| \phi_0 \right\rangle \\ &= - \frac{9g^4}{2k^3}, \\ \Delta E_0^{(4)c} &= g^4 \left\langle \phi_0 \left| \sigma^m \frac{-1}{k} \sigma^n \frac{-1}{2k} \sigma^m \frac{-1}{k} \sigma^n \right| \phi_0 \right\rangle \\ &= \frac{3g^4}{2k^3}, \\ \Delta E_0^{(4)d} &= g^4 \left\langle \phi_0 \left| \sigma^m \frac{-1}{k} \sigma^m \frac{1}{k} \sigma^n \frac{-1}{k} \sigma^n \right| \phi_0 \right\rangle \\ &= \frac{9g^4}{k^3}. \end{aligned} \quad (\text{A11})$$

We have obtained the formula for  $\Delta E_0^{(4)d}$  by using the rule established in Sec. IV A; i.e., the divergent energy denominator corresponding to the single-fermion intermediate state has been replaced (in this case) by the negative of the energy denominator for the preceding

fermion-gluon intermediate state. The sum of these fourth-order effects is seen to agree with the value obtained earlier in this appendix and demonstrates how our approach amounts to a rewording (or, more properly, a reshuffling) of the usual language.

- 
- [1] R. L. Jaffe, Phys. Rev. Lett. **38**, 195 (1977).  
 [2] P. Zenczykowski, Phys. Rev. D **36**, 3517 (1987).  
 [3] S. Takeuchi and M. Oka, Phys. Rev. Lett. **66**, 1271 (1991).  
 [4] B. A. Shahbazian, V. A. Sashin, A. D. Kechechyan, and A. S. Martynov, Phys. Lett. B **235**, 208 (1990).  
 [5] J. F. Donoghue, E. Golowich, and B. R. Holstein, Phys. Rev. D **34**, 3434 (1966).  
 [6] T. Sotirelis, Ph.D. thesis, University of Massachusetts, 1991.  
 [7] J. F. Donoghue and K. S. Sateesh, Phys. Rev. D **38**, 360 (1989).  
 [8] E. Golowich and E. Haqq, Phys. Rev. D **24**, 2495 (1981).  
 [9] R. D. Carlitz, S. D. Ellis, and R. Savit, Phys. Lett. **68B**, 443 (1977).  
 [10] F. E. Close and R. G. Roberts, Z. Phys. C **8**, 57 (1981).  
 [11] R. E. Cutkosky and R. E. Forsyth, Nucl. Phys. **B178**, 35 (1981).  
 [12] For an application of the time-evolution operator to a model of the quark-antiquark sea, see J. F. Donoghue and E. Golowich, Phys. Rev. D **15**, 3421 (1977).  
 [13] J. Goldstone, Proc. Soc. R. London **A239**, 267 (1957).  
 [14] The four-gluon “loop” diagram of Fig. 2(d) which contributes to a gluon line is poorly estimated in the truncation and is more a topic for study of renormalization than of phenomenology.  
 [15] For definiteness, these values correspond to the strange-quark mass  $m_s = 0$ .  
 [16] As a check, our  $O(\alpha_s^1)$  energy shift is found to be in accord with the value cited by Jaffe [1] once a similar set of bag parameters is used.  
 [17] G. Martinelli, in *Proceedings of the International Europhysics Conference on High Energy Physics*, Madrid, Spain, 1989, edited by F. Barreiro and C. Lopez [Nucl. Phys. B Proc. Suppl. **16**, 16 (1990)].  
 [18] T. Yoshié, in *Panic '87*, Proceedings of the Eleventh International Conference on Particles and Nuclei, Kyoto, Japan, 1987, edited by S. Homma *et al.* [Nucl. Phys. **A478**, (1988)].  
 [19] K. Maruyama, in *Panic '87* [18], p. 523.  
 [20] T. A. DeGrand, R. L. Jaffe, K. Johnson, and J. Kiskis, Phys. Rev. D **12**, 2060 (1975).  
 [21] D. Kastor and J. Traschen, Phys. Rev. D **44**, 3791 (1991).